

Coronary Artery Tracking from Dynamic Cardiac CT Sequences

Dong Ping Zhang^{a*}, Ose Pedro^a, Kensaku Mori^b, Philip Edwards^{a,c} and Daniel Rueckert^a

^aDepartment of Computing, Imperial College London, UK

^bGraduate School of Information Science, Nagoya University, Japan

^cDepartment of Biosurgery and Surgical Technology, Imperial College London, UK

Abstract. In this paper, we present an algorithm for coronary artery segmentation and tracking in dynamic cardiac CT sequences. The algorithm allows the automatic construction of a 4D coronary motion model from pre-operative CT which can be used for guiding totally-endoscopic coronary artery bypass surgery (TECAB). The A* graph search algorithm is used for tracking the coronary arteries through different time frames automatically. First, a Hessian-based vesselness filter is used to enhance tubular-like structure in the cardiac CT images. Then a smooth window function is used to highlight the intensity region where the coronaries appear. A cost function is constructed based on vesselness and intensity information. A common problem in dynamic cardiac CT is reconstruction artifacts occurring due to the cardiac and respiratory motion. To enable the tracking of the coronaries in these cases we use prior probability information from previous time frames to increase the robustness of the tracking. We have validated the accuracy of the proposed tracking algorithm by comparing the automatically tracked centerlines of the coronaries in each time frame with the manually extracted coronary centerlines. The average error of the tracking is 0.82mm for CT sequences I, 0.85mm for CT sequences II.

1 Introduction

As one of the leading causes of sudden death nowadays, coronary artery disease occurs due to the failure of the coronary circulation to supply adequate oxygen and nutrition to the myocardium and surrounding tissue. The typical cause of this insufficient supply is the built-up of plaque and fatty deposits in the artery walls, narrowing the vessels. To relieve this risk, arteries or veins grafted from patient's body are used to bypass the blockages and improve the supply to the heart muscle. Conventional bypass surgery requires invasive sternotomy and the use of a cardiopulmonary bypass, which leads to long recovery period for the patient and has high infectious potential. Totally endoscopic coronary artery bypass (TECAB) surgery based on image guided robotic surgical approaches have been developed to allow the clinicians to conduct the bypass surgery off-pump with only three pin holes incisions in the chest cavity, through which two robotic arms and one stereo endoscopic camera are inserted. However, the restricted field of view of the stereo endoscopic images leads to possible vessel misidentification and coronary artery mis-localization. This results in 20-30% conversion rates from TECAB surgery to the conventional invasive surgical approach [1–3].

In this work, we aim to construct a patient-specific 4D coronary artery motion models from preoperative dynamic cardiac CT scans. Through temporally and spatially aligning this model with the intraoperative endoscopic views of the patient's beating heart, this has the potential to assist the surgeon to identify and locate the correct coronaries during the robotically-controlled TECAB procedures.

Previous work on coronary tracking has focused on X-ray angiography. For example, Shechter et al [4–6] tracked coronary artery motion through a temporal sequence of biplane X-ray angiography images. A 3D Coronary model is reconstructed from extracted 2D centrelines in end-diastole angiography images. Registration based motion tracking algorithm is designed to recover the set of deformations along the cardiac cycle. An advantage of the proposed approach here is the fact that no 3D reconstruction from X-ray images is required in order to perform 3D coronary motion tracking. This simplifies the 4D motion modelling of coronaries significantly.

2 Method

A 4D motion model of the heart and the coronary arteries is needed for guiding the robotic TECAB procedure. This is achieved by segmenting the coronaries and the left ventricle from each time frame in dynamic CT image sequences. The resulting patient-specific motion model can then be used to augment the intraoperative images acquired with stereo-endoscope of the daVinci robot.

*Department of Computing, Imperial College London, London SW7 2AZ, UK. E-mail: dongping.zhang05@imperial.ac.uk

2.1 Multi-scale Vessel Enhancement

A coarse segmentation of the coronaries arteries in CT images is performed using a multiscale Hessian-based vessel enhancement filter [7]. The filter utilizes the 2nd-order derivatives of the image intensity after smoothing (using a Gaussian kernel) at multiple scales to identify bright tubular-like structures. The six second-order derivatives of the Hessian matrix at each voxel are computed by convolving the image with second-order Gaussian derivatives at pre-selected scale value.

Assuming a continuous 3D image function $I(p)$, the Hessian matrix at a given voxel p at scale σ is denoted as $H_\sigma(p)$. Let $|\lambda_1| \leq |\lambda_2| \leq |\lambda_3|$ denote the eigenvalues of the matrix $H_\sigma(p)$ and $\vec{v}_1, \vec{v}_2, \vec{v}_3$ are the corresponding eigenvectors. The principal curvature directions are then given by \vec{v}_2 and \vec{v}_3 . Since the coronaries appear as bright tubular structure surrounded by dark soft tissue in CT images, each vessel centre point corresponds to a local intensity maximum in the plane defined by the corresponding eigenvectors \vec{v}_2 and \vec{v}_3 . Thus, both λ_2 and λ_3 for a vessel point should be negative. We use the vesselness definition for voxel p at scale σ as proposed by Frangi et al. [7]

$$V(p, \sigma) = \begin{cases} 0 & \text{if } \lambda_2 > 0 \text{ or } \lambda_3 > 0 \\ \left(1 - \exp\left(-\frac{A^2}{2\alpha^2}\right)\right) \exp\left(-\frac{B^2}{2\beta^2}\right) \left(1 - \exp\left(-\frac{2C^2}{\gamma^2}\right)\right) & \text{otherwise} \end{cases} \quad (1)$$

where

$$A = \frac{|\lambda_2|}{|\lambda_3|}, \quad B = \frac{|\lambda_1|}{\sqrt{|\lambda_2\lambda_3|}}, \quad C = \sqrt{\lambda_1^2 + \lambda_2^2 + \lambda_3^2}$$

The parameter A is designed to distinguish between the plate-like and line-like structures. B reflects the deviation from blob-like structure and parameter C differentiates regions with high contrast from low contrast background. The parameters α, β, γ control the sensitivity of the tubular filter to A, B and C in the above equation. For parameter selections, we refer to Lindeberg et al [8]. In our experiments, we set the parameters $\alpha = 0.5, \beta = 0.5$ whereas γ is chosen as the largest norm of the eigenvalues across the whole image. The vesselness response is computed at four different scales, namely $\sigma = 0.5, 1, 2, 4$. The maximum response of the vesselness filter at the corresponding optimal scale is computed for each voxel of the image. The calculated vesselness image is used to facilitate the coronary extraction and tracking.

2.2 Prior Information for Coronaries Tracking in Dynamic CT

In some frames of the dynamic CT, the coronaries are difficult to extract. This is especially true in those phases during the cardiac cycle in which the heart is rapidly contracting or expanding. To allow the reliable extraction of the coronary arteries in these frames we have developed a framework which provides prior information about the location and shape of the coronary arteries in these frames. The basic idea of using prior information for tracking is that the location and shape of the coronary arteries is likely to be similar in subsequent frames. Thus, we are using the extracted coronary centrelines from frame t to assist the extraction in next frame $t + 1$. We define the prior probability of a voxel in time frame $t + 1$ to be part of the coronaries as a Gaussian probability P distribution centred at the voxel locations of the coronaries in time frame t . The parameter σ is chosen depending on the amount of motion between time frames: If the motion is rapid a large value of σ is chosen, if the motion is less rapid a small value of σ can be chosen.

In order to improve the estimate of the prior probability described above we additionally estimate the cardiac motion between time frames and then transform the prior probability using this transformation. In our case the cardiac motion between two adjacent frames is obtained from non-rigid image registration using a free-form deformation model based on cubic B-splines [9]. The motion is modelled using the following cubic B-spline model:

$$T(x, y, z) = \sum_{l=0}^3 \sum_{m=0}^3 \sum_{n=0}^3 B_l(u) B_m(v) B_n(w) \phi_{i+l, j+m, k+n} \quad (2)$$

A series of registration steps is performed to register each time frame to its subsequent time frame. The non-rigid registration algorithm optimizes normalised cross correlation as similarity measures between time frames. A gradient descent optimization is used to find the optimal transformation. Using the resulting transformation the prior probability information is propagated from each time frame to the subsequent time frame.

2.3 Coronaries Tracking Using the A* Graph Search algorithm

The A* graph search algorithm [10] is implemented to find the minimum cost path from a starting node S to an ending node E . The pair of nodes S and E are supplied by the user in each frame. The uni-directional graph search algorithm evaluates the smallest cost from node S to current node x denoted as $g(x)$ and the heuristic cost from current node to node E denoted as $h(x)$ to determine which voxel to be searched next. The search algorithm finds the optimal path only if the heuristic underestimates the cost. Euclidean distance from x to E is used to calculate the heuristic cost in our application. The heuristic measurement we used is guaranteed to be lower than true optimal path cost.

Since the multiscale vessel enhancement only measures local contrast without taking the surrounding region information into account, a smooth window based on the Gaussian error function erf is constructed to identify and highlight the intensity regions containing coronaries [11].

$$W(p) = \frac{1}{2}(erf(b(I(p) - a_1)) + 1)(1 - \frac{1}{2}(erf(b(I(p) - a_2)) + 1)) \quad (3)$$

where a_1 is the estimation of lowest intensity value for a voxel along the coronaries, a_2 is the highest one. The parameter b controls the steepness of the smoothing window. Using eq. (3) and combining this with the vesselness filter defined in the previous section, we define the cost CI as, for each voxel p as:

$$CI(p, \sigma) = \frac{1}{V(p, \sigma)(W(p))^\kappa + \epsilon} \quad (4)$$

where $V(p, \sigma)$ is the vesselness of voxel p at the optimal scale as described in section 2.1. Parameter κ controls the influence of W . ϵ is a small positive constant added in to avoid the singularities.

To automatically extract the coronaries from the CT sequences with varied image qualities, we additionally add the prior information. We evaluate the score $g(x)$ as:

$$g(x) = g(x') + CI(x) * (|\ln(P(x))|)^\eta. \quad (5)$$

where parameter η defines the importance of prior information for tracking in current frame. To initialize the cost function, $g(x')$ for the starting node S is set to be zero. $P(x)$ is the prior probability for voxel x from section 2.2.

The whole cost function for assessing each candidate node is defined as

$$f(x) = g(x) + \frac{\delta h(x)}{2} \quad (6)$$

where δ is estimated as the ratio of the minimum cost of the vessel to the Euclidean distance of the starting and ending nodes in the previous time frame. By using the heuristic term, the searching space greatly is reduced and the minimum cost path can be found in real-time. When node E is reached and it also has lower f function value than any other candidates in the searching queue, the minimum cost path is reconstructed by tracing backwards to node S .

The minimum cost path detection algorithm results in a discrete path consisting of an ordered set of discrete locations (voxels). After extraction of the path we estimate a B-spline representation of the centreline of the coronaries which smoothly approximates these voxel locations.

3 Results and Evaluation

3.1 Coronary Artery Extraction

Coronary arteries are extracted with A* graph search algorithm from several CT sequences. The first dataset is ten-phased cardiac sequences, with image dimensions $512 \times 512 \times 231$ voxels, voxel dimension $0.62 \times 0.62 \times 0.5$ mm. It has minor artifacts due to the reconstruction errors when rapid cardiac motion occurs. This enable us to use graph search with the vesselness based approach to automatically extract the LAD, LCX and RCA with a single pair of start and end nodes for each branch of the coronaries. The parameters for the dataset are selected as: $a_1 = 1100$, $a_2 = 1500$, $b = 0.1$, $\kappa = 0$, $\eta = 0$. δ is initialized to 10 for the first time frame.

We have also tested the algorithm on another dataset which is characterized by more severe artifacts, in particular along the right coronary and left circumflex. Dataset II has ten time frames, with image dimension $512 \times 512 \times 298$

voxels, voxel dimension $0.36 \times 0.36 \times 0.5$ mm. Prior coronary models were constructed for each frame in Dataset II to incorporate with probability approach. The parameters are chosen as $a_1 = 1000, a_2 = 1450, b = 0.1, \kappa = 1, \eta = 1, \delta = 0$. Heuristic is used in both approaches to reduce the searching time. Figure 1 shows two image slices and their coronary extractions from the CT sequences. The rectangles mark out the region of interest.

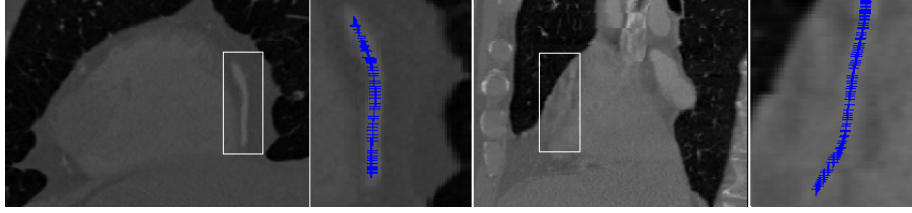


Figure 1. CT Image and Coronary Artery. From left to right, (1) CT slice from dataset I. (2) extracted coronary from (1). (3) CT slice with severe artifacts from dataset II. (4) extracted coronary from (3).

The automatically tracked 3D coronary centerlines from second dynamic CT sequences are shown in Fig. 2. The red lines denote the right coronary artery, the green lines denote the left anterior descending and its branches and the blue lines denote the left circumflex artery and its branches.

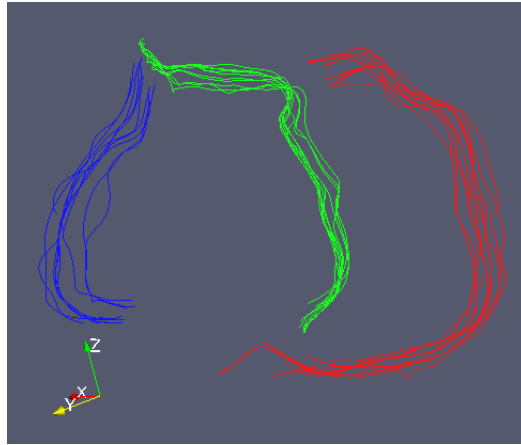


Figure 2. Automatically Extracted Coronary Arteries

3.2 Coronary Motion Model and its Evaluation

In order to assess the quality of automatic extraction results, the distance between the manual segmentations M and automatic extractions U of the coronaries in each time frame is measured. The distance is defined as

$$D(M, U) = \frac{1}{N_M} \sum_{i=1}^{N_M} \|m_i - l(m_i, U)\|_2 + \frac{1}{N_U} \sum_{j=1}^{N_U} \|u_j - l(u_j, M)\|_2 \quad (7)$$

where N_M and N_U are the number of points representing vessel M and vessel U correspondingly. For each point $m_i \in M$, $l(m_i, U)$ calculates the closest point of m_i on the automatically extracted vessel U . Similarly, for each point $u_j \in U$, $l(u_j, M)$ defines the closest point of u_j on the vessel M .

By automatically tracking the coronaries from each timeframe in CT sequences, the coronary motion model can be formed. The amount of deformation of the coronaries during the cardiac cycle can be quantitatively measured by computing the distance between the centerlines at current frame and in the end-diastole timeframe I_1 using Equation 7.

4 Discussion and Future Work

We have presented a novel approach for patient-specific coronary artery tracking and motion modeling from dynamic cardiac CT images to assist the totally endoscopic coronary artery bypass surgery. The proposed method has been tested on the clinical CT datasets acquired from two subjects. By constructing a 4D motion model of coronaries from pre-operative cardiac images and aligning the 4D coronary model with the series of 2D endoscopic images capture

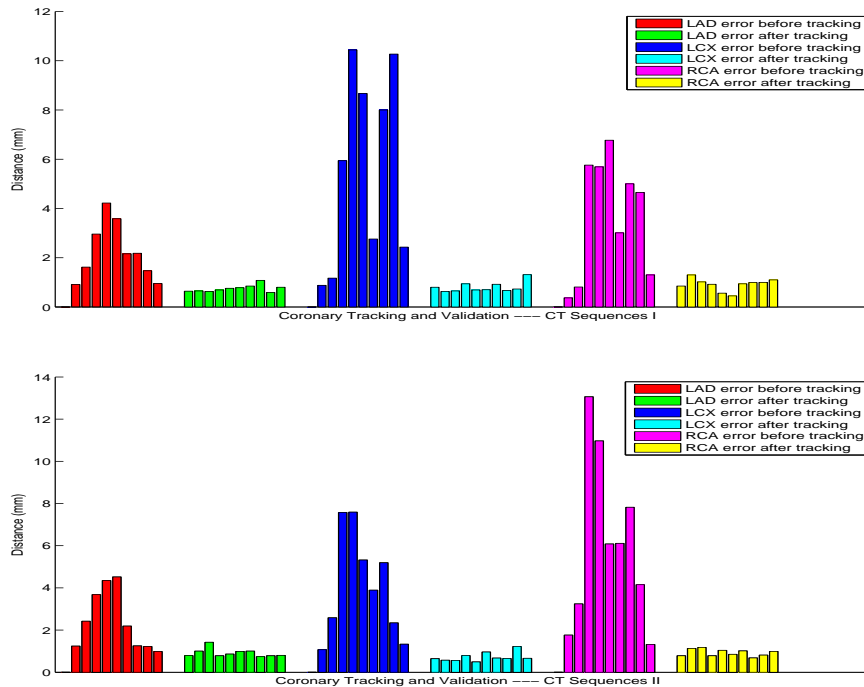


Figure 3. The coronary error before tracking is measured as the distance between the automatically extracted centreline at end-diastole of the cardiac cycle and all the other automatic extractions in the rest timeframes. The error after tracking is calculated as the distance between the manual and automatic segmentation for each coronary artery in each of the ten frames.

during the operation, we aim to assist the surgical planning and provide image guidance in robotic-assisted totally endoscopic coronary artery bypass (TECAB) surgery. Through this work, we expect to reduce the conversion rate from TECAB to conventional invasive procedures.

References

1. F. W. Mohr, V. Falk, A. Diegeler et al. "Computer-enhanced "robotic" cardiac surgery: Experience in 148 patients." *Journal of Thoracic and Cardiovascular Surgery* **121**(5), pp. 842 – 853, 2001.
2. U. Kappert, R. Cichon, J. Schneider et al. "Technique of closed chest coronary artery surgery on the beating heart." *European Journals of Cardio-Thoracic Surgery* **20**, pp. 765–769, 2001.
3. S. Dogan, T. Aybek, E. Andressen et al. "Totally endoscopic coronary artery bypass grafting on cardiopulmonary bypass with robotically enhanced telemanipulation: Report of forty-five cases." *Journals of Thoracic Cardiovascular Surgery* **123**, pp. 1125–1131, 2002.
4. G. Shechter, F. Devernay, E. Coste-Maniere et al. "Temporal tracking of 3D coronary arteries in projection angiograms." In *Proc. SPIE Medical Imaging*, volume 4684, pp. 612–623. 2002.
5. G. Shechter, F. Devernay, A. Quyyumi et al. "Three-dimensional motion tracking of coronary arteries in biplane cineangiograms." *IEEE Transactions in Medical Imaging* **22**(4), pp. 493–603, 2003.
6. G. Shechter, J. R. Resar & E. R. McVeigh. "Displacement and velocity of the coronary arteries: cardiac and respiratory motion." *IEEE Transactions on Medical Imaging* **25**, pp. 369–375, 2006.
7. A. Frangi, W. Niessen, R. Hoogeveen et al. "Model-based quantitation of 3D magnetic resonance angiographic images." *IEEE Transactions on Medical Imaging* **18**(10), pp. 946–956, 1999.
8. T. Lindeberg. "Feature detection with automatic scale selection." *International Journal of Computer Vision* **30**, pp. 79–116, 1998.
9. D. Rueckert, L. I. Sonoda, C. Hayes et al. "Nonrigid registration using free-form deformations: application to breast MR images." *IEEE Transactions on Medical Imaging* **18**(8), pp. 712–721, 1999.
10. P. E. Hart, N. J. Nilsson & B. Raphael. "A formal basis for the heuristic determination of minimum cost paths." *Systems Science and Cybernetics, IEEE Transactions on* **4**(2), pp. 100–107, 1968.
11. C. Metz, M. Schaap, T. van Walsum et al. "Two point minimum cost path approach for CTA coronary centerline extraction." *Midas Journal - 2008 MICCAI Workshop - Grand Challenge Coronary Artery Tracking 2008*.